Biosensors and Bioelectronics 66 (2015) 512–519

Contents lists available at ScienceDirect

Biosensors and Bioelectronics

journal homepage: www.elsevier.com/locate/bios

Real-time monitoring of mycobacterium genomic DNA with target-primed rolling circle amplification by a Au nanoparticle-embedded SPR biosensor

Yang Xiang [a], Xiaoyan Zhu [b], Qing Huang [b], Junsong Zheng [a,*], Weiling Fu [b,*]

[a] Department of Clinical Laboratory Science, Southwest Hospital, Third Military Medical University, Chongqing 400038, China
[b] Department of Laboratory Medicine, Southwest Hospital, Third Military Medical University, Chongqing 400038, China

ARTICLE INFO

Article history:
Received 20 August 2014
Received in revised form
13 November 2014
Accepted 14 November 2014
Available online 18 November 2014

Keywords:
Target-primed rolling circle amplification
Surface plasmon resonance
Real-time monitoring
Au nanoparticle-embedded
Mycobacterium

ABSTRACT

In this study, we developed a surface plasmon resonance (SPR) DNA biosensor array based on target-primed rolling circle amplification (RCA) for isothermal and rapid detection of two pathogenic mycobacteria, *Mycobacterium tuberculosis* complex (MTBC) and *Mycobacterium avium* complex (MAC).The species-specific padlock probe (PLP) was designed to target the sequence in 16S–23S rRNA gene internal transcribed spacer (ITS). After ligation, the circularized PLP could be primed by the target sequence to initial RCA. The RCA performed simultaneously with the cleavage reaction to produce small fragments of single strand DNA which immediately hybridized with the probe immobilized on the sensor chip without denaturation. This process caused SPR angle changes on the chip surface, which made the detection for analysis from the solution achievable, and dynamic real-time RCA monitoring of mycobacterium possible. Besides, Au nanoparticles (AuNPs) were directly assembled onto the surface of the sensor chip via hexanedithiol (HDT) for the enhancement of sensitivity as a label-free detection system. Experimental results show that the signal enhancement by the target-primed RCA together with AuNPs-embedded surface caused at least10-fold increased sensitivity as compared with conventional RCA on bare SPR chip method. Within 40 min amplification duration as low as 20 amol of synthetic targets and 10^4 CFU mL^{-1} of genomic DNA from clinical samples can be detected. The proposed method not only provides a simple design idea for liquid-phase amplification monitoring, but also apply it in clinical pathogen detection, which holds great promise in ultrasensitive bioassay in the future.

1. Introduction

Mycobacterium tuberculosis complex (MTBC) and *Mycobacterium avium* complex (MAC) are both genus *Mycobacterium*. MTBC causes tuberculosis (TB) which is still a global pandemic resulting insignificant morbidity and mortality. MAC belongs to non-tuberculous mycobacterium (NTM), which is an opportunistic pathogen causing tuberculosis-like lesions, and has been identified as the second leading cause of death among HIV-positive patients (Sharma et al., 2012). Unlike MTBC, MAC has its own resistance pattern. The routine anti-TB treatment to the patients with MAC infected would induce drug-resistance and lead to the failure of treatments. Therefore, it is important to distinguish TB from NTM disease by the pathogen detection. The conventional TB test relies on sputum smear microscopy and culture-based methods, which is time-consuming and highly false-negative. Rapid identification of pathogenic bacteria can make earlier initiation of correct antimicrobial therapy possible at a lower cost. The recently developed molecular biology techniques based on nucleic acid or antibody, such as immunofluorescence (Kim et al., 2012), real-time PCR (Causse et al., 2011), microarray method (Jia et al., 2012), improve the sensitivity and specificity, but are laborious, expensive, requiring sophisticated equipment and trained personnel. Thus, it is necessary to develop a new diagnostic method that is easily applicable to allow specific and sensitive detection pathogens from clinical samples.

Nucleic acid amplification is one of the most useful tools in clinical diagnosis. So far, a number of new methods and technologies have been invented based on the polymerase chain reaction (PCR) with high sensitivity. However, it also has drawbacks such as the nonspecific amplification and non-compatibility with on-chip amplification. Alternatively, recent developments in biotechnology offer a wide variety of choices for nucleic acid amplification, among which rolling circle amplification (RCA) is an increasingly popular isothermal replication technology with high specificity

* Corresponding authors. Fax: +86 23 65460909.
E-mail addresses: zhengalpha@yahoo.com (J. Zheng), weilingfu@yahoo.com (W. Fu).

http://dx.doi.org/10.1016/j.bios.2014.11.021
0956-5663/

and simplicity (Mothershed and Whitney, 2006). Conventional RCA is a polymerase based reaction initiated by the circular template and its primer, which generates a long ssDNA product comprised of thousands of tandem repeats and complementary to the circular template. As an isothermal amplification technology, RCA does not require temperature cycling instruments, which makes it special suitable for on-chip detection. By now, the target quantitative analyses in many RCA-based assays have been achieved by the quantification of the RCA products, such as the fluorescence measurement, the nanoparticle based detection and the enzyme linked assay (Li et al., 2010; Su et al., 2011; Wang et al., 2014). However, most approaches need labeling, complicated surface functionalization chemistry or multiple treatment processes.

Surface plasmon resonance (SPR) is an optical detection technique that uses the reflection and refraction of light. SPR biosensor is a surface-sensitive analytical technique based on the ability to detect changes in the refractive index that are caused by the interaction between an analyte and a biological recognizer immobilized on the biosensor surface (Homola, 2008). Although, combined with the intrinsic sensitivity of optical transduction, many studies on the SPR-based pathogenic microorganism detection could not achieve lower detection limit without pre-amplification (Boozer et al., 2006; Duman and Piskin, 2010; Lecaruyer et al., 2006; Rachkov et al., 2011; Stapleton et al., 2009). On the other hand, in the most of the on-chip based SPR detections, surface associated amplification or nano-tag probes are applied to achieve higher sensitivity (He et al., 2014; Hu and Zhang, 2010). However, according our previous study, the nucleic acid amplification on solid surface is poor in chip regeneration and less reaction efficiency compared to liquid-phase (Shi et al., 2014; Xiang et al., 2013). If a new SPR method could be developed to real-time monitor RCA in liquid-phase, many advantages could be achieved, such as dynamic real-time detection, higher sensitivity, less time consuming, resistant to contamination, lower power consumption, markedly simplified procedure and suitable for multiplexing.

In view of the fact that gold nanoparticles (AuNPs) are the promising nanomaterials explored for chemical and biological sensing application, because AuNPs are easy preparation, inert nature, favorable biocompatibility, high surface area, and especially suitable for binding of bimolecular due to thiol–gold association. AuNPs-coupled SPR biosensors have been investigated to enhance the detections system, because AuNPs are known to induce a considerable shift in the angle of plasmon resonance. However, the direct labeling of nanoparticle to probes entails cumbersome multi-step procedures and disrupts the accurate measurement of kinetic constants, resulting in loss of the SPR advantage in terms of label-free detection. AuNPs can excite the surface plasmons to particle plasmons when nanoparticles are embedded on the Au film. The AuNPs-based nanostructures formed by a AuNPs monolayer depositing on a Au surface, can lead to strong optical coupling of incident light to resonances, thus enhance the sensitivity of a SPR biosensor (Chen et al., 2004).

Herein, the current study is directed to the development of a new biosensor method to rapidly and accurately identify two common pathogenic mycobacteria in parallel, through the integration of liquid RCA reaction and SPR assay. The liquid-phase RCA-cleavage reaction was designed to perform in the detection cell inside the biosensor, which generated considerable small ssDNA fragments immediately hybridizing with the probes immobilized on the sensor surface without denaturation. Besides, we directly assembled AuNPs onto SPR chip surface instead of labeling them with probes in order to enhance the SPR signal as a label-free detection system. The SPR angle change caused by the refractive index change on the sensing membrane corresponds to the RCA process. Thus, the liquid-phase RCA reaction can be dynamically real-time monitored in a label-free manner. The sensitivity and specificity of the SPR biosensor method were evaluated and the method was applied to the detection of clinical samples.

2. Experimental

2.1. Reagents and materials

The oligonucleotides (Table 1) were synthesized by Sangon Biotech (Shanghai, China). *Escherichia coli* DNA ligase, bovine serum albumin (BSA), and DNA ladder markers (100–1000 bp) were from TaKaRa (Dalian, China). *HhaI* restriction enzyme and the mixture of deoxyribonucleoside triphosphates (dNTPs) were from Fermentas (USA). *Phi29* DNA polymerase and exonuclease I were purchased from New England Biolabs (USA). AuNPs with an average diameter of 15 nm were purchased from JY Biotech (Shanghai, China). Hexanedithiol and dimethyl sulfoxide were from Sigma Aldrich (St. Louis, MO, USA). Standard bacterial strains *M. tuberculosis* (ATCC 27294), *M. avium* (ATCC25291) and *Streptococcus pneumoniae* (ATCC 49619) with inactivation were from the National Institute for the Control of Pharmaceutical and Biological Products, China. Buffers used in the study: ligation buffer (30 mM Tris–HCl pH 7.8, 4 mM $MgCl_2$, 10 mM $(NH_4)_2SO_4$, 1.2 mM EDTA, 0.1 mM NAD) and RCA-cleavage reaction buffer (0.2 $\mu g\ \mu L^{-1}$ BSA, 5% DMSO, 50 mM Tris–HCl, 10 mM $MgCl_2$, 10 mM $(NH_4)_2SO_4$, 4 mM DTT, pH 7.5) were prepared. All chemicals were analytical reagent grade and used as received.

The "P" represents a phosphate at the 5′ end for ligation. MTBC target 2 is the single-base mismatch sequence compared to MTBC target 1, and the mismatched nucleotide is underlined. The bold bases in PLP sequences mean phosphorothioates.

2.2. Apparatus

The SPR biosensor modified by our laboratory including a polarized light detection system, a sample-loading chamber, a microflow pump, a temperature control system and a four-channel circulating detection cell was made by Cyto Trend Biotech Engineering (Beijing, China). Glass prisms coated with 50nm-thick gold film on the upside were obtained from GP Medical Technologies (Beijing, China). The detection cell was in negative pressure

Table 1
Sequences of oligonucleotides used in this study.

Oligonucleotide	Sequence (5′→3′)
MTBC target 1	GAGAGCCGGGTGCATGACAACAAAGTTGGCCACCAACACAC
MTBC target 2	GAGAGCCGGGTGCATGACAACAGAGTTGGCCACCAACACAC
MAC target	GGCCCTGAGACAACACTCGGTCCGTCCGTGTGGAGTCCCTCC
PLP of MTBC	P–TGTTGTCATGCACCCGGGTCTATATGTCTGTGCGACCTCAGCATCGACCT**GCGC**ATTTTTAGTACTATGGTGGCCAACTT
PLP of MAC	P–GACGGACCGAGTGTTGTGTCTATATGTCTGCAGCATCGGACCGGTAATCG**GCGC**ATTTTTAGTACTAGGGACTCCACACG
Probe of MTBC	TGCGACCTCAGCATCGACCT$(T)_{20}$–$(CH_2)_6$–HS
Probe of MAC	CAGCATCGGACCGGTAATCG$(T)_{20}$–$(CH_2)_6$–HS

to form a sealed condition to assure the stability of the system during reaction. The resolution of the scan angle was 0.55 m° (milli-degree).

2.3. Fabrication of the AuNPs-embedded SPR sensor chip

A self-assembled monolayer (SAM) of hexanedithiol (HDT) was performed by immersing a clean Au-coated chip (50 nm-thick) glass prism into a freshly made 2 mM of HDT ethanol solution for 24 h at room temperature. After absorption, the Au chip modified with HDT was thoroughly rinsed with ethanol and deionized water to remove physically adsorbed HDT. Then, the HDT-modified Au chip was exposed to a 10-fold diluted solution of colloidal AuNPs in deionized water for 30 min in darkness at room temperature to fabricate the monolayer of AuNPs on the HDT-modified chip surface. After washing with deionized water, the AuNPs-assembled SPR chip was dried with nitrogen gas (Moon et al., 2006). A field emission scanning electron microscopy (LEO SUPRA 35; Oberkochen, Germany) was employed to analyze the surface morphology to make sure the AuNPs uniformly distributed over the chip surface.

The probe was respectively immobilized onto the two different channels of the same SPR sensor chip through the thiol method to form the sensing membrane with nanostructure.

2.4. Target-primed rolling circle amplification

Firstly, 10 μL reaction buffer containing 0.1 μM linear PLP and targets in interest were incubated at 40 °C with 2 U of *E. coli* DNA for 30 min. After exonucleolysis by exonuclease I, the RCA-cleavage reaction was conducted by addition of 1 U μL^{-1} *Phi29* DNA polymerase, 1 U μL^{-1} *HhaI* endonuclease and 1 mM dNTPs. For clinical samples, the genomic DNA was denatured for 3 min in a boiling water bath and immediately cooled in ice water before detection.

2.5. SPR real-time detection

The system was kept at 40 °C, and RCA reaction buffer was piped into detection cell to equilibrate the chip surface. Then, the RCA-cleavage reaction mixture was added to perform the amplification in the detection cell, which generated a large amount of small ssDNA fragments directly hybridizing to the probes immobilized on the chip. The SPR angle value was recorded all through the amplification reaction. Under the excitation wavelength of 650 nm, any change in the refractive index caused by both the nucleic acid amplification and hybridization were monitored in real time and converted into electrical signals that were used to analyze the concentration of the targets.

3. Results and discussion

3.1. Operation principle and basic reaction style

The basic response mode of SPR biosensor is that the mass of the molecules binding on the gold surface varies proportionally to the refractive index change on the sensor surface. In this detection, the liquid-phase RCA reaction was performed in the detection cell and real-time monitored by SPR sensor. To improve the sensitivity, HDT was used as a chemical linker for the formation of a monolayer of AuNPs to produce an active interface on the SPR chip surface, which yielded increased surface area for site-specific binding and the transduction of small refractive index change on the sensing chip (Choi et al., 2008; Sanvicens et al., 2009). For that the products of RCA are long and large nucleotide fragments, easily form random cross-linking coils in solution and hinder the hybridization, the RCA products need to be digested into small fragments before hybridization on chip (Nilsson et al., 2002; Smolina et al., 2004). However, to maintain a continuous reaction and monitor the complete amplification process, RCA and digestion reaction were designed to perform simultaneously. The sequence of 5′-GCGC-3′in ssDNA can be recognized by *HhaI*, through the transiently formed double-stranded hairpin structures at a relatively fast reaction speed (Reckmann and Krauss, 1987). According to this, we designed the cutting-site into the PLP sequence to produce a large amount of repeated cutting-sites (5′-GCGC-3′) in RCA products. Meanwhile, in order to protect the circular PLP from cleaving during the digestion, the cutting-site in the PLP was phosphorothioated (Dean et al., 2001). Fig. 1A illustrates the principle of the target-primed RCA-cleavage reaction-based AuNP-embedded SPR assay. Upon the hybridization of PLP and its matched target, the two ends of PLP are joined through ligation, locking the probe onto the target molecule. RCA is initiated by turning the target molecule into a primer through 3′–5′exonucleolysis of free 3′end of the target strand protruding beyond the probe-recognition site. Combined with cleavage reaction by the restriction endonuclease, the RCA can generate small ssDNA fragments that directly hybridize with immobilized probes without denaturation. Each PLP contains a unique code sequence, an enzyme cutting site, and two specific target-complementary sequences (Fig. 1B). When RCA is primed by the target, the generated ssDNA sequence hybridize to the immobilized probes via the unique code sequence recognition resulting in refractive angle changes respectively, which are recorded in a real-time manner and proportional to the target mass.

The typical SPR angle change during real-time monitoring of the liquid-phase RCA by the modified SPR biosensor is shown in Fig. 2. The reaction was triggered by the target samples, and an enormous number of single-strand nucleic acid chains capable of binding to probes immobilized on the gold films of the sensors were generated by the extension, displacement and cleavage. The fundamental angle (S_0) of the gold film was recorded when a steady angle was obtained. Though the mass change would alter the surface refraction index, biomacromolecules such as enzymes and nucleic acids in the RCA system were expected to undergo sudden movement such as mass transfer and exchange, which would result in a dramatic change in the density and viscosity of the reaction mixture (Park et al., 2007; Yamasaki et al., 2006). The surface refraction index of the SPR sensor was not only sensitive to the mass change on the surface of the gold film but also highly sensitive to the changes in the properties of the reaction substance (non-mass change). The coexistence of mass and non-mass changes on the surface of the SPR sensor led to a slow rise (S_1) during the early stage of the reaction for that the non-mass change was larger in the beginning. Only after the reaction had lasted for a certain time that sufficient nucleic acid chains were generated to maintain a steady angle increase on the sensor surface (S_2). When the angle increased to the extent that the probes were consumed, it resulted in the plateau stage (S_3). During the whole process, the SPR signal stability of the blank channel (control) with buffer alone was achieved with a signal range of ± 6.7 m°, which compared to the signal change of the positive channel ($S_3 - S_0$) was significant ($p < 0.05$). Therefore, combined with the stable and sensitive SPR sensor system, making use of the specially designed PLP, and integrating with the properties of enzyme reactions, we propose here a new strategy for SPR detection of pathogenic mycobacterium.

3.2. Optimizing the reaction condition

3.2.1. Effect of hybridization temperature

The ligation reaction, especially the hybridization between the

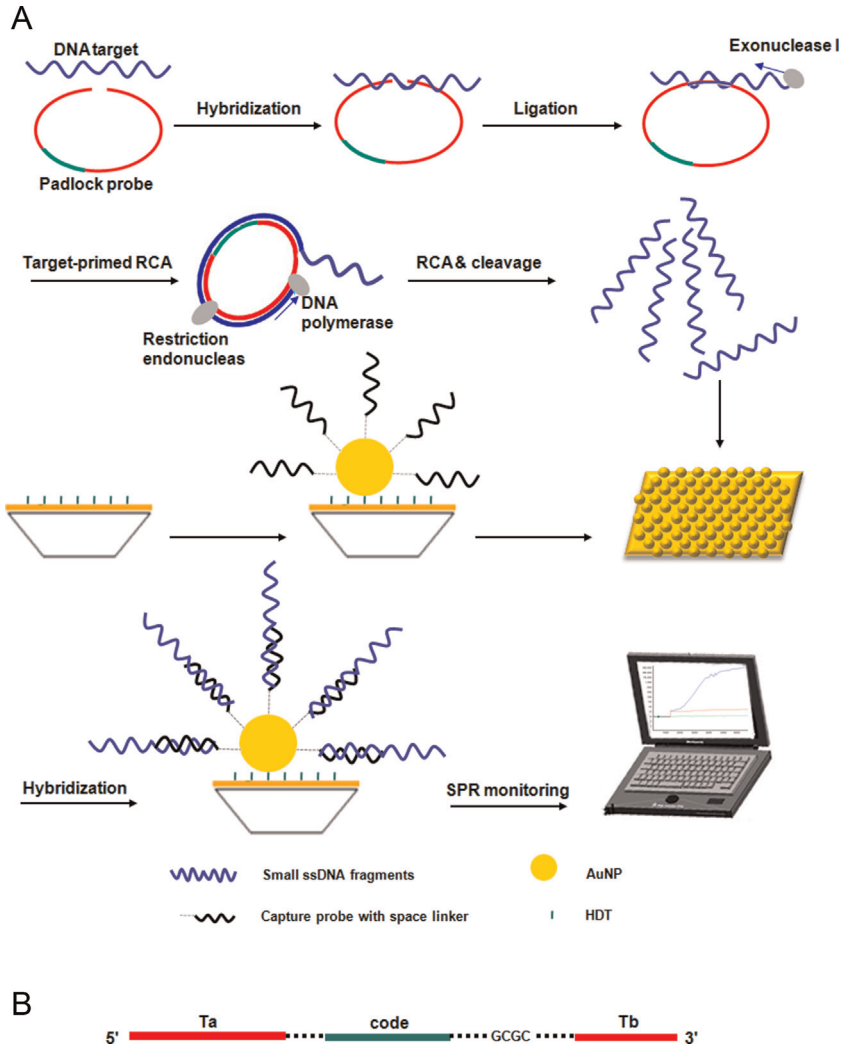

Fig. 1. (A) The principle of the target-primed RCA-cleavage reaction-based AuNP-embedded SPR assay. (B) The mode of the padlock probe. Ta and Tb are asymmetric target complementary regions in the PLP. Each PLP contains a unique code sequence for multiplex hybridization. The dotted line represents the bases in the linker sequence.

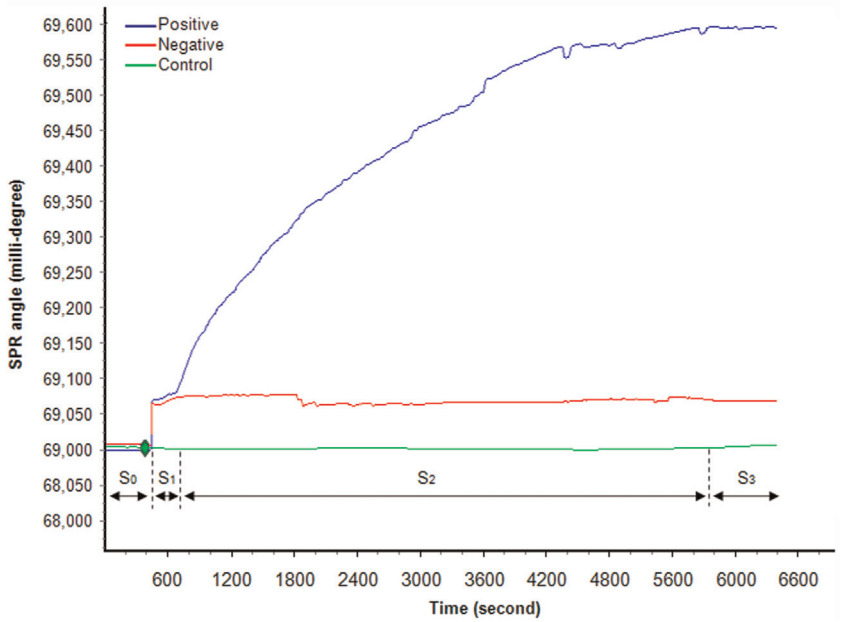

Fig. 2. The real-time RCA-SPR monitoring diagram of the MTBC genomic DNA. The negative curve resulted from MAC. The concentration of PLP and the target was 0.1 μM and 10 nM, respectively.

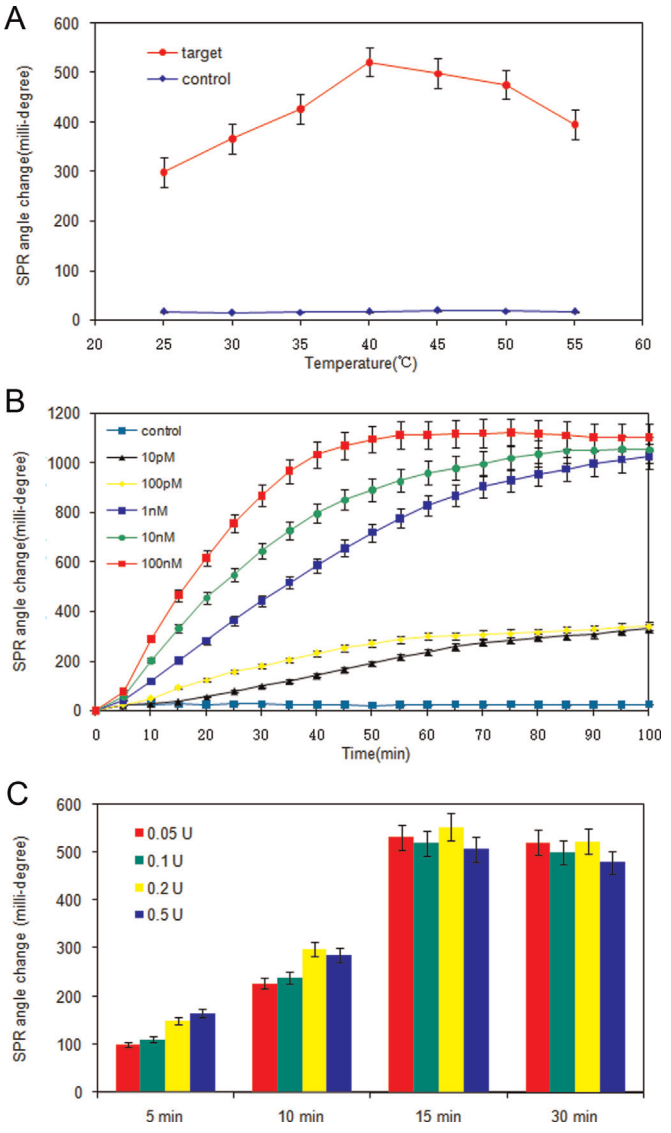

Fig. 3. Optimization of experiment conditions. (A) Hybridization temperature on SPR angle change. (B) The amplification time versus SPR angle change with various initial target concentrations. (C) Effect of exonuclease I on SPR angle change. The concentration of PLP and the target was 100 nM and 1 nM, respectively in all experiments. Error bars indicate the standard deviation ($n=5$).

two termini of PLP and the target, is the key to successful detection. A suitable hybridization temperature should be determined to minimize the second structure in linear PLP and ensure the efficiency and specificity of the ligation reaction. Herein, a series of hybridization temperatures, varying from 25 °C to 55 °C with an interval of 5 °C, were investigated. As presented in Fig. 3A, the maximum SPR signal of positive target was observed at 40 °C, which was between the melting temperature of the two termini of PLP (Szemes et al., 2005). When the hybridization temperature continued to increase, the SPR angle changed unnoticeably. The value of the control was always low and hardly changed in detection period. Hence, 40 °C was chosen as the hybridization temperature in all the following experiments.

3.2.2. *Effect of RCA-cleavage reaction time*

A careful choice of the reaction time endpoint is critical for the liquid-phase RCA-based SPR method. Since, the length of DNA strand generated from RCA is proportional to the reaction time, and the refractive index change is proportional to the mass of products bound on the sensor chip surface, one would expect a larger SPR angle change from longer reaction time. However, as the result showed in Fig. 3B, if the amplification time is too long, the angle changes for various DNA initial concentration approach similar values, thus it is difficult to distinguish between two different initial concentrations. On the other hand, for too a short reaction time, the angle change of low initial concentration is too small to detect. To establish the optimal reaction time we analyzed the correlation coefficients between the initial concentrations of DNA targets and the angle change at varying amplification times. We used a linear curve fitting of different endpoint data to find the maximum correlation coefficients of the response curves, which are listed in appendix (Table 1). It was found that the time of around 40 min could get the maximum correlation coefficient ($R^2=0.957$). These results demonstrated that the analysis can provide more rapid but also quantitative detection of amplification.

3.2.3. *Effect of exonuclease*

During the target-primed RCA, the target strand can first act as a template for circularizing the linear PLP and then prime RCA. This approach can avoid topological inhibition, increase replication efficiency and simplify the operation as well (Cheng et al., 2008; Larsson et al., 2004). Though, any 3′ end strand of the target that protrudes beyond the probe-recognition site can be removed by the 3′→5′ exonucleolytic activity of the *Phi29* polymerase, until the enzyme can use the circularized probe to template the RCA reaction, it is found that the longer distance of the free 3′ end of the target to the probe-recognition site, the less dominance of the enzyme in polymerase activity (Larsson et al., 2004). Furthermore, the excess unlighted PLP would hinder the hybridization on the sensor chip and decrease the detection efficiency. Exonuclease I degrades only ssDNA in a strict 3′→5′ direction (Hafner et al., 2001). To ensure the 3′ end of target close to the probe-recognition site, which was required to initiate more efficient target-primed RCA, we used exonuclease I to remove the free 3′ end strand protruding beyond probe-recognition site and remove the excess linear oligonucleotides. However, to maintain a sealed reaction system, exonuclease I was directly added to the system along with RCA mixture. To avoid suppressing the amplification followed, optimizing of the exonuclease reaction was necessary. Various concentrations of exonuclease I and incubation time were evaluated against the SPR angle changes as shown in Fig. 3C. The concentration of 0.2 U μL^{-1} exonuclease I was found to produce the best amplification effect. A higher concentration of exonuclease I decreased the SPR signal, which might be attributed to the degradation of linear products. A lower concentration also decreased the signal, probably because the excess linear oligonucleotides would hinder the hybridization reaction, or that the 3′–5′ exonucleolytic activity of the *Phi29* polymerase was in dominance leading to the reduced DNA yield. The influence of the exonuclease reaction time was also studied. As shown, by increasing the reaction time up to 15 min, SPR signal increased and then leveled off for longer reaction time. Therefore, 0.2 U μL^{-1} of exonuclease I and 15 min were proposed as the optimum exonuclease reaction condition for detection.

3.3. *Specificity of detection*

To evaluate the specificity of the method, we compared the SPR angle changes caused by MTBC target DNA with those caused by mismatched oligonucleotide strands. Corresponding control experiments (in the absence of target DNA) were performed under the same condition as negative control. The targets were from MTBC, MAC and single-base mismatch of MTBC with the same concentration of 100 pM. The results indicated that the SPR angle change from MTBC targets (350.6 ± 22.6 m°) was significantly

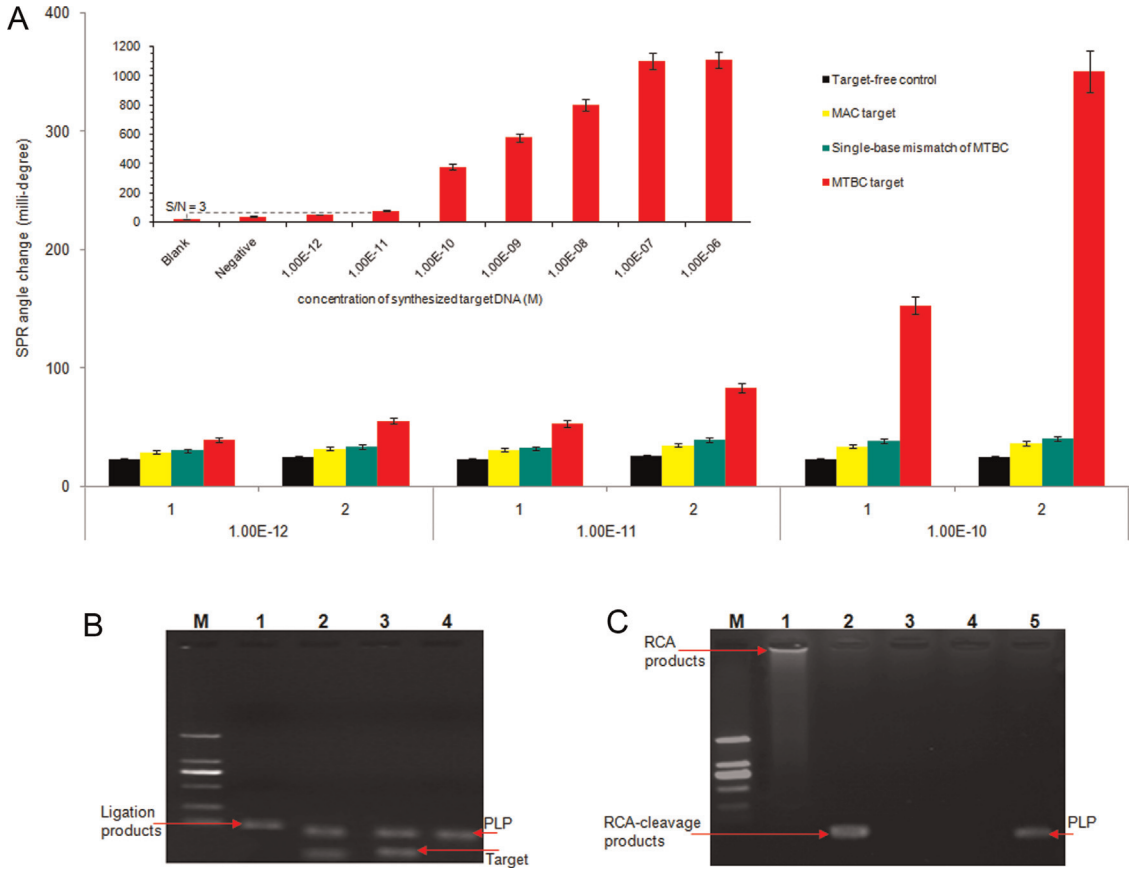

Fig. 4. (A) Comparison of SPR angle changes of the two methods (1: the conventional RCA on bare chip; 2: the target-primed RCA on AuNPs-embedded chip) with specific and nonspecific targets at different concentrations. The inset displays angle change on the *y*-axis and the increase of MTBC concentration on the *x*-axis. The dashed line represents the threshold value. Error bars were estimated from five replicate measurements. (B) Electrophoresis identification of the enzymatic ligation reaction. Lanes 1, 2, 3 and 4 represent the ligation products from MTBC, single-base mismatch of MTBC, MAC and target-free control, respectively. (C) Electrophoresis identification of RCA and its cleavage products. Lanes 1 and 2 represent the RCA and RCA-cleavage products from MTBC target, respectively; lanes 3 and 4 represent the products from single-base mismatch of MTBC, MAC target, respectively; and lane 5 represents the bands of PLP. The nucleotides analyzed in electrophoresis had a concentration of 0.5 μM.

higher than that of MAC targets (36.1 ± 4.6 m°) and single-base mismatch of MTBC (40.4 ± 2.3 m°) demonstrating that the proposed method can distinguish non-specific target even single-base mismatch, due to the high specificity of ligation and hybridization reaction (Fig. 4A). The small angle change observed from the mismatched target could be attributed to the limited RCA-free extension of mismatched strands from the unligated PLP (Banér et al., 2001; Yao et al., 2013).

We also verified the specificity of the ligation reaction by the characteristic electrophoretic migration in 1% agarose gel electrophoresis. In Fig. 4B it was observed that the linear PLP (80bp) ligated to circular only in the presence of MTBC targets, and that the linear moved a little faster than the circular. The products of RCA reaction were analyzed by electrophoresis as well. In Fig. 4C the polymerization products (lane 1) were too large to enter the gels, but the identity was achieved by restricting digestion to small fragments (lane 2) with the same size to that of PLP (lane 5). This verified that the RCA products were composed of multiple repeated copies of PLP. The results demonstrated that the small ssDNA could be produced in a specific sequence-dependent manner and the ligation reaction was highly specific for single-base discrimination, which indicated the high specificity of the presented method.

3.4. Sensitivity of detection

To evaluate the sensitivity of this method, we investigated the relationship between the concentration of ITS gene from MTBC and the SPR angle change. As shown in the inset of Fig. 4A, the SPR angle change increased when the target concentration increased. The blank control and the negative control (10^{-9} M DNA target from MAC) were also tested, but yield angle barely changes. The SPR angle change versus the logarithm of target concentration showed linearity in the range from 10^{-11} M to 10^{-7} M ($y = 241.0x + 2739$, $R^2 = 0.993$). The detection limit was estimated as 1×10^{-11} M (about 20 amol target sequence) with S/N = 3. Therefore, it features close to attomolar sensitivity. When the target concentration was further increased to 10^{-6} M, no significant increase in the SPR signal was observed ($p > 0.05$). The reason might be that the probes immobilized on the chip surface were saturated, or that high mass transfer rates within the medium were directed to the sensor surface (due to high concentration difference – "the driving force"), which prevented complete hybridization and caused less mass accumulation (means low relative refractive index) (Homola, 2008). To investigate the precision of the proposed assay, relative standard deviation (RSD) was determined by measuring SPR signal in different concentrations with five replicates. The RSD values for all concentrations were less than 10% suggesting an acceptable reproducibility. The sensitivity was 4 orders lower than that of the directly detected *M. tuberculosis* using SPR biosensor without amplification (Duman and Piskin, 2010), also superior to the sensitivity of detection on bare chip as well as the conventional ligation-RCA based electrochemical detection previously reported (Yi et al., 2014; Zhang et al., 2009).

Furthermore, the sensitivity of the target-primed RCA on AuNPs-embedded SPR chips and conventional RCA on bare chip

for detection of MTBC target was compared in order to investigate the signal enhancement. As observed in Fig. 4A, the signal from the target-primed RCA on AuNPs-embedded chip at the concentration of 10^{-11} M was 83.1 m°, whereas it did not reach the threshold value with conventional RCA on bare chip, and neither reached the threshold value at the concentration of 10^{-12} M. However, the former resulted in a 161% higher SPR signal increase compared to the latter at the concentration of 10^{-10}, which was compatible with the 10-fold enhancement in the detection sensitivity. This enhanced sensitivity was probably due to the following facts: first, the higher reaction efficiency from the target-primer RCA avoiding the process of primer annealing to the circular template; second, the design of performing RCA and enzyme digestion simultaneously to generate small ssDNA fragments that could directly hybrid with probes without denaturation; third, the coupling of the localized surface plasmon of the AuNPs with the propagating plasmon in the Au chip surface enhanced the SPR signal change in bimolecular interactions (Ko et al., 2009; Lyon et al., 1998). Besides, the AuNPs-based nanostructure on the chip surface increased the sensing membrane area for site-specific binding of bimolecular and reduced the steric hindrance of hybridization.

3.5. Detection of bacterial genomic DNA

After proving the specificity and sensitivity of the target-primed RCA based SPR method, we applied it to detect genomic DNA from *M. tuberculosis* and *M. avium* with the above optimization. Serially diluted genomic DNA (10^3–10^9 CFU mL^{-1}) was analyzed to obtain the response SPR angle change. As shown in Fig. 5A, the detection limit of *M. tuberculosis* and *M. avium* were 4.2×10^4 CFU mL^{-1} (0.005 ng μL^{-1}) and 3.7×10^4 CFU mL^{-1} (0.002 ng μL^{-1}), respectively, as the SPR angle changes were 98 ± 10.1 m° and 89.4 ± 8.2 m°. The linearity of SPR angle was observed from 10^4 CFU mL^{-1} to 10^8 CFU mL^{-1} with a regression coefficient of 0.987 for *M. tuberculosis* and 0.983 for *M. avium*. We expected this analytical sensitivity of our proposed method to be sufficient for detecting mycobacterium genomic DNA from clinical samples. This sensitivity was comparable with or even exceeded the DNA-based detection platforms reported previous, such as the gold nanoparticle based colorimetric detection (1.875 ng μL^{-1}) (Liandris et al., 2009), the helicase amplification detection with electrochemistry (0.01 ng μL^{-1}) (Torres-Chavolla and Alocilja, 2011), and the nanoparticle-based SPR detection (7×10^5 CFU mL^{-1}) (Joung et al., 2008). Even though there were reported loop-mediated isothermal amplification (Lamp), quantitative PCR and PNA-based methods for *M. tuberculosis* detection with higher sensitivity (Li et al., 2014; Prabhakar et al., 2008; Sales et al., 2013), the RCA-SPR method proposed in this study provided a label-free, real-time monitoring, cost-effective and low power consumption detection without the complicated primers design or the possibility of high false positive rate.

Cross-reaction was also investigated between the target and non-specific probes to evaluate the selectivity of the method for application to multiplex detection in clinical samples. The tested genomic DNA was from *M. tuberculosis*, *M. avium* and *S. pneumoniae* with concentrations of 10^6 CFU mL^{-1}. Multiplex detection was performed by adding the two PLPs (final concentration 0.1 μM) in the mixed samples. As shown in Fig. 5B, the difference in the SPR angle change between the specific and non-specific pairs was significant which meant the non-specific cross-reaction was very low. This is mainly attributed to the unique code

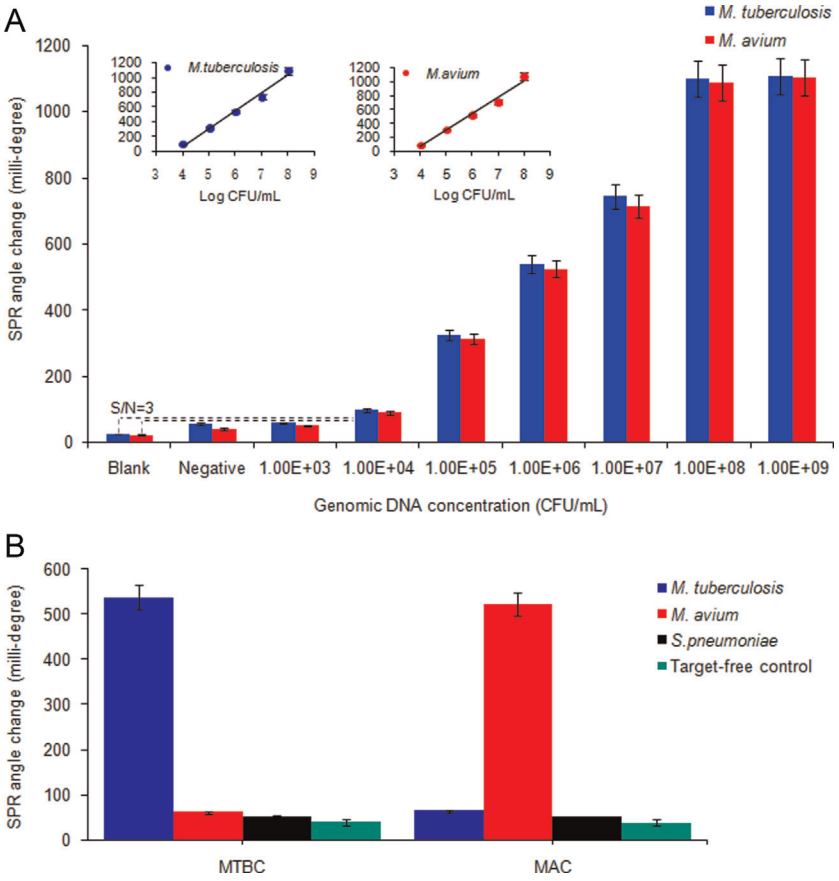

Fig. 5. (A) The sensitivity assessment of RCA SPR method applied to genomic DNA detection. (B) Cross-reaction of the *M. tuberculosis*, *M. avium* and *S. pneumoniae* genomic DNA detected by the RCA SPR method. The dashed line represents the threshold value. Error bars indicate the standard deviation ($n=5$).

sequence carried in the PLP with a similar length and melting temperature values while self-pairing or hairpin was eliminated was complementary to the probe immobilized on the sensor chip. That ensured the hybridization can be performed in the same condition as well as high selectivity.

We further detected genomic DNA from clinical samples including sputum, urine and cerebrospinal fluid by the proposed method, and verified it by PCR (appendix 2). Among 24 cases of positive clinical samples, one sample was inconsistence with the PCR method, which was mostly due to the failure of DNA extraction or the low concentration of target DNA (less than 10^4 CFU mL^{-1}) in the samples. All the negative samples showed consistent results by both methods. The result demonstrated that the developed method could be successfully used for mycobacterium detection of real genomic DNA from clinical samples.

4. Conclusions

The target-primed rolling circle amplification in liquid-phase can be real-time monitored with AuNPs-embedded SPR sensing method, which is achieved to multiple detection of mycobacterium genomic DNA via hybridization analysis of ITS gene. The new method takes advantage of the specificity of padlock probes, the simplicity of target-primed RCA, the combination of RCA and digestion reaction, and the enhanced sensitivity of AuNPs-embedded SPR sensor, providing improved detection limit with high fidelity. Because the real-time RCA monitoring allows a closed-tube diagnostic format, it also minimizes the risk of false-positive results via cross-contamination and simplifies operations. Furthermore, the proposed method detects target by measuring the refractive index difference capable of achieving real-time label-free monitoring of nucleic acid amplification at constant temperature to amplify DNA to a detectable level, which is more time-efficient, lower power consumption and less volume of sample used. Considering these merits, it will find more potential for application of variety of biorelated markers in genetic research and field diagnosis in third world countries.

References

Banér, J., Nilsson, M., Isaksson, A., Mendel-Hartvig, M., Antson, D.O., Landegren, U., 2001. Curr. Opin. Biotechnol. 12, 11–15.
Boozer, C., Kim, G., Cong, S.X., Guan, H.W., Londergan, T., 2006. Curr. Opin. Biotechnol. 17 (4), 400–405.
Causse, M., Ruiz, P., Gutiérrez-Aroca, J.B., Casal, M., 2011. J. Clin. Microbiol. 49 (8), 3065–3067.
Chen, S.J., Chien, F.C., Lin, G.Y., Lee, K.C., 2004. Opt. Lett. 29 (12), 1390–1392.
Cheng, Y., Li, Z., Zhang, X., Du, B., Fan, Y., 2008. Anal. Biochem. 378, 123–126.
Choi, S.W., Kim, H.S., Kang, W.S., Kim, J.H., Cho, Y.J., Kim, J.H., 2008. J. Nanosci. Nanotechnol. 8 (9), 4569–4573.
Dean, F.B., Nelson, J.R., Giesler, T.L., Lasken, R.S., 2001. Genome Res. 11 (6), 1095–1099.
Duman, M., Piskin, E., 2010. Biosens. Bioelectron. 26 (2), 908–912.
Hafner, G.J., Yang, I.C., Wolter, L.C., Stafford, M.R., Giffard, P.M., 2001. BioTechniques 30 (4), 852–867.
He, P., Liu, L., Qiao, W., Zhang, S., 2014. Chem. Commun. 50 (12), 1481–1484.
Homola, J., 2008. Chem. Rev. 108 (2), 462–493.
Hu, J., Zhang, C.Y., 2010. Anal. Chem. 82 (21), 8991–8997.
Jia, K., Yu, M., Zhang, G.H., Zhang, J., Lin, Z.X., Luo, C.B., Yu, H.Q., Li, S.J., 2012. J. Vet. Diagn. Investig. 24 (1), 156–160.
Joung, H.A., Lee, N.R., Lee, S.K., Ahn, J., Shin, Y.B., Choi, H.S., Lee, C.S., Kim, S., Kim, M. G., 2008. Anal. Chim. Acta 630, 168–173.
Kim, J.H., Yeo, W.H., Shu, Z., Soelberg, S.D., Inoue, S., Kalyanasundaram, D., Ludwig, J., Furlong, C.E., Riley, J.J., Weigel, K.M., Cangelosi, G.A., Oh, K., Lee, K.H., Gao, D., Chung, J.H., 2012. Lab Chip 12 (8), 1437–1440.
Ko, S., Park, T.J., Kim, H.S., Kim, J.H., Cho, Y.J., 2009. Biosens. Bioelectron. 24, 2592–2597.
Larsson, C., Koch, J., Nygren, A., Janssen, G., Raap, A.K., Landegren, U., Nilsson, M., 2004. Nat. Methods 1 (3), 227–232.
Lecaruyer, P., Mannelli, I., Courtois, V., Goossens, M., Canva, M., 2006. Anal. Chim. Acta 573-574, 333–340.
Li, J., Deng, T., Chu, X., Yang, R., Jiang, J., Shen, G., Yu, R., 2010. Anal. Chem. 82, 2811–2816.
Li, Y., Shi, L., Pan, A., Cao, W., Chen, X., Meng, H., Yan, H., Miyoshi, S., Ye, L., 2014. J. Microbiol. Methods 104, 55–58.
Liandris, E., Gazouli, M., Andreadou, M., Comor, M., Abazovic, N., Sechi, L.A., Ikonomopoulos, J., 2009. J. Microbiol. Methods 78 (3), 260–264.
Lyon, L.A., Musick, M.D., Natan, M.J., 1998. Anal. Chem. 70 (24), 5177–5183.
Moon, J., Kang, T., Oh, S., Hong, S., Yi, J., 2006. J.Colloid Interface Sci. 298 (2), 543–549.
Mothershed, E.A., Whitney, A.M., 2006. Clin. Chim. Acta 363, 206–220.
Nilsson, M., Gullberg, M., Dahi, F., Szhuai, K., Raap, A.K., 2002. Nucl. Acids Res. 30 (14), e66.
Park, H., Germini, A., Sforza, S., Corradini, R., Marchelli, R., Knoll, W., 2007. Biointerphases 2 (2), 80–88.
Prabhakar, N., Arora, K., Arya, S.K., Solanki, P.R., Iwamoto, M., Singh, H., Malhotra, B. D., 2008. Analyst 133 (11), 1587–1592.
Rachkov, A., Patskovsky, S., Soldatkin, A., Meunier, M., 2011. Talanta 85 (4), 2094–2099.
Reckmann, B., Krauss, G., 1987. Biochim. Biophys. Acta 908 (1), 90–96.
Sales, M.L., Fonseca Jr., A.A., Orzil, L., Alencar, A.P., Hodon, M.A., Issa, M., Soares Filho, P.M., Silva, M.R., Lage, A.P., Heinemann, M.B., 2013. Genet. Mol.Res. 13 (2), 4607–4616.
Sanvicens, N., Pastells, C., Pascual, N., Marco, M.P., 2009. TrAC-Trend Anal. Chem. 28 (11), 1243–1250.
Sharma, K., Sharma, A., Modi, M., Singh, G., Kaur, H., Varma, S., Sharma, M., 2012. J. Med. Microbiol. 61, 1789–1791.
Shi, D., Huang, J., Chuai, Z., Chen, D., Zhu, X., Wang, H., Peng, J., Wu, H., Huang, Q., Fu, W., 2014. Biosens. Bioelectron. 62, 280–287.
Smolina, I.V., Demidov, V.V., Cantor, C.R., Broude, N.E., 2004. Anal. Biochem. 335 (2), 326–329.
Stapleton, S., Bradshaw, B., O'Kennedy, R., 2009. Anal. Chim. Acta 651 (1), 98–104.
Su, H., Yuan, R., Chai, Y., Mao, L., Zhuo, Y., 2011. Biosens. Bioelectron. 26 (11), 4601–4604.
Szemes, M., Bonants, P., de Weerdt, M., Baner, J., Landegren, U., Schoen, C.D., 2005. Nucl. Acids Res. 33 (8), e70.
Torres-Chavolla, E., Alocilja, E.C., 2011. Biosens. Bioelectron. 26 (11), 4614–4618.
Wang, D.C., Hu, L.H., Zhou, Y.H., Huang, Y.T., Li, X.H., Zhu, J.J., 2014. J. Biomed. Nanotechnol. 10 (4), 615–621.
Xiang, Y., Deng, K., Xia, H., Yao, C., Chen, Q., Zhang, L., Liu, Z., Fu, W., 2013. Biosens. Bioelectron. 49, 442–449.
Yamasaki, R., Kim, J., Jung, H., Lee, H., Kawai, T., 2006. Biochem. Eng. J. 29 (1), 125–128.
Yao, C., Xiang, Y., Deng, K., Xia, H., Fu, W., 2013. Sens. Actuators B-Chem. 181, 382–387.
Yi, X., Li, L., Yi, P., Guo, L., 2014. Biosens. Bioelectron. 57 (15), 103–109.
Zhang, S., Wu, Z., Shen, G., Yu, R., 2009. Biosens. Bioelectron. 24 (11), 3201–3207.